

Original Article

# Energy and Exergy-Based Modeling and Performance Evaluation of a Natural Gas-Fired Combined-Cycle Power Plant

Bijay Kumar Roy<sup>1</sup>, Reeta Sharma<sup>2</sup>, Deva Kanta Rabha<sup>3</sup>

<sup>1,2,3</sup>Mechanical Engineering Department, Jorhat Engineering College, Jorhat, Assam, India.

<sup>1</sup>Corresponding Author : [sriroybk@gmail.com](mailto:sriroybk@gmail.com)

Received: 08 May 2024

Revised: 07 June 2024

Accepted: 06 July 2024

Published: 30 July 2024

**Abstract** - This paper utilizes operational data to demonstrate the energy and exergy analysis of a 100MW combined cycle power plant. The primary objective of this paper is to examine the various components of the cycle to identify and measure the particular locations with the greatest amount of destruction and to determine the effectiveness of all components. Furthermore, the study also examines the impact of ambient temperature, compression ratio, and turbine inlet temperature. A comprehensive thermodynamic model of the entire cycle has been formulated by employing mass, energy, and exergy balance equations. The thermodynamic parameters at the inlet and outlet conditions of the components, as well as the energy, exergy losses, and efficiencies, are determined using the Engineering Equation Solver (EES) software. According to the energy analysis results, the condenser is responsible for the highest amount of energy loss, accounting for 35.72% of the total energy supplied. However, exergy analysis reveals that the main sources of irreversibilities are the combustion chamber, gas turbine, Heat Recovery Steam Generator (HRSG) and steam turbine, which account for 37.08%, 4.26%, 3.89%, and 3.33% of the total exergy supplied, respectively. The overall exergy and energy efficiency of the combined cycle are 47.25% and 49.24%, respectively.

**Keywords** - Energy, Exergy, Efficiency, Irreversibility, Combined cycle power plant.

## 1. Introduction

Energy consumption is increasing globally daily due to the expansion of manufacturing and industries, rapid urbanization, the development of domestic appliances, and population growth. Therefore, energy generation must be increased to meet the present demand for energy. A combined-cycle power plant has drawn much attention due to its high thermal efficiency, lower environmental impact, and economical power generation compared with an individual gas turbine or “steam turbine cycle. The Brayton and Rankine cycles, which comprise these power plants, are connected by an HRSG between the steam turbine (bottoming cycle) and gas turbine (topping cycle). Additionally, the exhaust gas from the gas turbine is used by the HRSG to produce steam, which runs a steam turbine and generates energy. An energetic analysis based on the first law of thermodynamics offers a metric for work capacity or quality. On the other hand, exergetic analysis estimates the quantity or maximum amount of work that can be done and is based on the second rule of thermodynamics [1]. Exergetic analysis also identifies the sources, locations, and exergy loss of irreversibilities in each system component. When designing, evaluating, optimizing, and improving thermal power plants, the exergetic technique is helpful [2–5]. In the last few years, a number of

investigations “have been performed to assess the performance of a combined cycle power plant utilizing energy and energy concepts. The majority of researchers use different operating parameters, like ambient temperature, compression pressure ratio, turbine inlet temperature, condenser pressure, gas turbine back pressure, air-fuel ratio, dryness fraction, humidity, etc., to study how well a combined-cycle power plant and its components perform [6-10].

Ibrahim Dincer and Yunus A. Cengel [1] introduced concepts of energy, entropy, and exergy that are relevant to all branches of science and engineering. They characterize thermodynamics as an entropy, energy, and exergy-related science. Energy analysis, which helps detect losses in work and possible gains or efficient use of resources, is governed by the first law of thermodynamics. However, the second law of thermodynamics, often known as exergy analysis, takes into consideration the entropy component by adding irreversibilities.

Ahmadi et al. (2) performed a 4E analysis and optimization to examine how well the Combined Cycle Power Plant (CCPP) performs. Their results show that the Combustion Chamber (CC) of the CCPP undergoes the



greatest exergy destruction and that as the temperature at the turbine inlet increases, the costs associated with exergy destruction decrease. The optimization process also suggests that environmental impacts can be reduced by minimizing the fuel flow rate in the CC and selecting the most efficient components.

Balku [4] employed natural gas to carry out the modeling, simulation, and optimization of combined cycle power plants. The simulation results indicate that the combustion chamber is an important component.

The outcomes of optimization indicate that the air-fuel and pressure ratios for the gas turbine and compressor are the most crucial factors in the production of power. With optimal design variables, the plant's thermal efficiency rises by 22.55% and loss of energy drops by 22.65%.

A triple-pressure combined cycle plant was optimized and subjected to exergoeconomic analysis by Bakhshmand et al. [5]. As per the exergoeconomic optimization results, the plant's energy and exergetic efficiencies increase by 3%, and its overall cost rate decreases by 9% at optimal design parameters.

Vandani et al. [6] investigated the impact of diesel instead of natural gas on a CCPP regarding exergetic, economic, and environmental impacts. They also optimized the cycle's performance for natural gas as well as diesel using a binary genetic algorithm.

The energy and exergy performance of a coal-based power plant's supercritical boiler under three distinct load scenarios was reported by Adibhalta and Kaushik [11]. They found that the turbine's rate of exergy destruction is significantly lower under sliding pressure than it is under constant pressure and that the boiler and turbine have the highest rates of exergy destruction under part load situations.

Ameri et al. [12] performed the irreversibility of each major component of a 420 MW combined cycle power plant using the exergy analysis. They discovered that the combustion chamber, gas turbine, duct burner, and heat recovery steam generator are the main causes of irreversibility, contributing more than 83% of the overall exergy losses. Because of its great irreversibility, the gas turbine's combustion chamber loses the most exergy. Without a duct burner, the CCPP has an exergy and thermal efficiency of 45.5% and 47%, respectively. The HRSG may increase the steam cycle's output power by utilizing a duct burner. Energy as well as exergy analysis was done for a combined cycle power plant by Cihan et al. [13] in order to see if system efficiency could be raised. Thus, energy and exergy fluxes and losses at each component's inlet and outlet locations were assessed. Their investigation revealed that combustion chambers, gas turbines, and HRSG are the primary sources of

irreversibilities, which account for more than eighty-five percent of total exergy losses.

In order to examine the behavior of operating parameters, Khaleel et al. [14] created an analytical model of a coal-based thermal power plant. They discovered that increasing the superheater pressure by 100% increased the net power delivered by the cycle by more than 8%. In a similar vein, increasing the temperature of the superheated steam from 539.8°C to 580°C increased the net power that the cycle produced by more than 6%.

Utilizing design data, Aliyu et al. [15] provided an energy and exergy analysis of a triple-pressure combined cycle power plant with reheat. The stack was the main source of energy destruction, with the steam turbine cycle's HRSG, turbine, and condenser coming in second and third. The condenser has the lowest energy efficiency in the STC, measuring about 63%, while the turbine has the highest energy efficiency, measuring over 92%. Parametric analysis shows that superheat pressure, reheat pressure, and steam quality at the turbine's exit affect output and efficiency.

An exergy analysis for various parts of a combined cycle power plant in Dadri, India, was presented by Tiwari et al. [16]. The results showed that, at 1400°C turbine inlet temperature and pressure ratio 10, the gas turbine combustion chamber accounted for thirty-five percent of the total exergy loss, while other plant components experienced exergy losses ranging from seven percent to twenty-one percent. Besides compression ratio and turbine inlet temperature, they showed exergy loss variations in the compressor, combustion chamber, gas turbine, and heat recovery steam generators.

An exergy analysis of the 180 MW Garri "2" combined cycle power station was conducted by Abuelnuor et al. [17]. Due to their high irreversibility, the data indicated that combustion chambers accounted for 63% of the overall exergy destruction. Gas turbines came in second with 13.6%, steam turbines with 6.4%, HRSG with 6.3%, and exhaust gases with 4.7% of the total exergy destruction. The thermal and exergetic efficiency for the plant is 38% and 49%, respectively.

Ersayin and Ozgener assessed combined-cycle power plant energy and exergy [18]. Energy efficiency was 56 percent, and exergy efficiency was 50.04 percent for the CCPP. The combustion chamber showed the highest rate of exergy destruction among all the system components. To increase the efficacy of the CCPP, they suggested a few modifications.

Aljundi [19] assessed the energy as well as exergy of an STPP in Jordan, along with the impact of reference environment temperature. He reported that approximately 66 percent of the energy input was lost to the cooling water in the

condenser, while the boiler's combustion chamber experienced the highest exergy destruction representing 77 percent. This was followed by 13% for the turbine and 9% for the condenser. The performance of the major components changed with reference environment temperature.

Sengupta et al. [20], utilizing design data at 100%, 75%, 60%, and 40% load conditions, assessed the performance of a 210 MW thermal plant. They found that the boiler is the main source of irreversibility in the power cycle, accounting for about sixty percent of the exergy destruction. Energy efficiency is reduced when the condenser back pressure rises. When the high-pressure heaters are gradually removed, the efficiency increases for the equipment excluding the boiler but decreases for the entire plant, including the boiler. Sustaining main steam pressure before turbine control valves in sliding mode enhances part-load energy efficiency.

A CCPP with a triple-pressure steam cycle that included reheating using energy and exergy was examined by Pattanayak et al. [21]. The effects of the surrounding temperature, the condenser, the exhaust pressure loss, the CCPP load, and the percentage of excess air were all examined. An increase in exhaust and inlet pressure loss, as well as a rise in compressor inlet air temperature, results in a decline in the combined cycle efficiency. The CCPP's total power output falls as ambient air temperature rises. The condenser, HRSG, and CC have exergy efficiency values of 29%, 87.20%, and 77.48%, respectively. The unit's overall energy and energy efficiency are found to be 54.09%, 58.26%, and 53.92%, 57.10%, respectively, at 100% design and operating condition. Improving the bottoming cycle losses can raise the total energetic efficiency of the CCPP.

Shamet et al. [22] presented the performance assessment obtained from the 2E analysis of Sudan's Garri 4 power plant. The boiler accounted for the largest portion of energy destruction (approximately 84.36%), according to the results. This percentage can be reduced by regulating the air-to-fuel ratio and warming the inlet water to an appropriate temperature. It was discovered that the condenser was the main cause of energy loss (approximately 67%).

Elhelw et al. [23] used exergy analysis to evaluate a 650 MW steam power plant at full and half load. They found that the boiler, turbine, and condenser lose the most energy. When condenser pressure is dropped from 0.067 to 0.049 bar, full and half load power reductions are 0.5725% and 0.5878%. Additionally, they demonstrated that raising the superheat temperature inlet to HPT and IPT is the optimal option because it reduces thermal stress, increases efficiencies with a sizable portion of power savings, and decreases energy losses.

Sanjay [24] examined how changes in operating parameters affected the gas-steam combined cycle's exergy destruction and rational efficiency. He demonstrated that the

overall rational efficiency of the steam turbine and gas turbine is higher at higher compressor pressure ratios and turbine input temperatures. The combustor exhibited the highest level of energy destruction, trailed by the compressor and gas turbine. Using a multi-pressure-reheat steam generator arrangement reduces the destruction of energy.

Khaldi and Adouane [25] employed Cycle-Tempo to conduct an exergy analysis to evaluate an Algerian gas turbine power plant. Under certain design, equipment specifications, and operational intake conditions, the plant's energy efficiency is 32.24%. Furthermore, it was established that the combustor, which consumes 58% of the exergy, is the primary exergy destroyer. More importantly, the power plant and its entire parts turbine excluded are less efficient when operating at 83% of full load, or off-design. Heating the air before it enters the combustor can greatly increase the plant's energy efficiency. Preheating the air to 800°C increases the plant's energy efficiency to 68%.

Kwak et al. [26] evaluated a 500 MW combined cycle power plant's energy and thermoeconomics. These assessments applied mass and energy conservation to every system component. System-wise and component specific quantitative energy and energetic cost balances were evaluated. Cost generation and component interaction were visualized utilizing the exergoeconomic model, which showed the system's productive structure. Power plant production costs can be determined through this study's computer program.

One of the primary issues, according to the literature on CCPPs, is losses that occur in the cycle's parts. It is critical to determine the cycle's contributing elements and the extent of the losses in order to improve the combined cycle's efficiency. The review of the literature revealed that there has not been any research on energy and energy analyses of power plants in northeastern India. Thus, to pinpoint the locations and components of the Namrup thermal power plant in Northeastern India that are causing significant thermodynamic losses and direct attention toward minimizing them, an energetic and exergoeconomic evaluation of the plant has been conducted.

## 2. Plant Description

Namrup Thermal Power Station (NTPS) is one of Assam's major gas-based power-generating stations situated in Namrup, Dibrugarh. It was established in 1965 with three GT units (3x23 MW). Another three units (GT-1x22.5 MW, ST-1x30 MW, and ST with HRSG-1x22.5 MW) were commissioned in 1975, 1976, and 1985, respectively. Due to aging and low performance, old units (unit-1, unit-4, and unit-5) of NTPS have been decommissioned and replaced by the Namrup Replacement Power Project (NRPP). Commissioned on July 16, 2021, the NRPP (Phase 1) is a 98.40 MW installed

capacity (GTG-62.25 MW + STG-36.15 MW) natural gas-fired CCGT.

Figure 1 displays the NRPP's layout diagram. The Compressor (C), Mixing Chamber (MC), feed water pumps (HPP, IPP and LPP), Deaerator (DEA), Gas Turbine (GT), Triple Pressure HRSG (HP, IP and LP), Triple Pressure Steam Turbine (HPST, IPST and LPST), Condenser (COND), Condensate Extraction Pump (CEP), Gland Steam Condenser (GSC), and Generator (GEN) are the principal parts of the system. Using an axial flow compressor, air at 306 K temperature and 1.01 bar pressure is compressed to 12.72 bar (18 stages) and then enters the reverse flow, can annular type combustion chambers equipped with six combustors. At 306 K temperature and 15.86 bar pressure, natural gas is injected

into the CC. At 1528 K temperature, the flue gas from the CC enters the three-stage impulse turbine. A triple-pressure HRSG uses the gas turbine's high temperature exhaust gas to produce steam. At 74.19 bar, the HP steam enters HPST and expands. The expanded steam of the HPST is mixed with the IP steam and enters the IPST at a pressure of 22.25 bar, where it is expanded. The expanded steam of the IPST is mixed with LP steam and enters the LPST at a pressure of 4.46 bar and then expands. The expanded steam from LPST is then condensed in a surface condenser. The condensate water is transported to the deaerator by CEP via gland steam condenser, mixing chamber and condensate pre-heater. Deaerator water is fed to the three sections of HRSG by HPP, IPP and LPP.

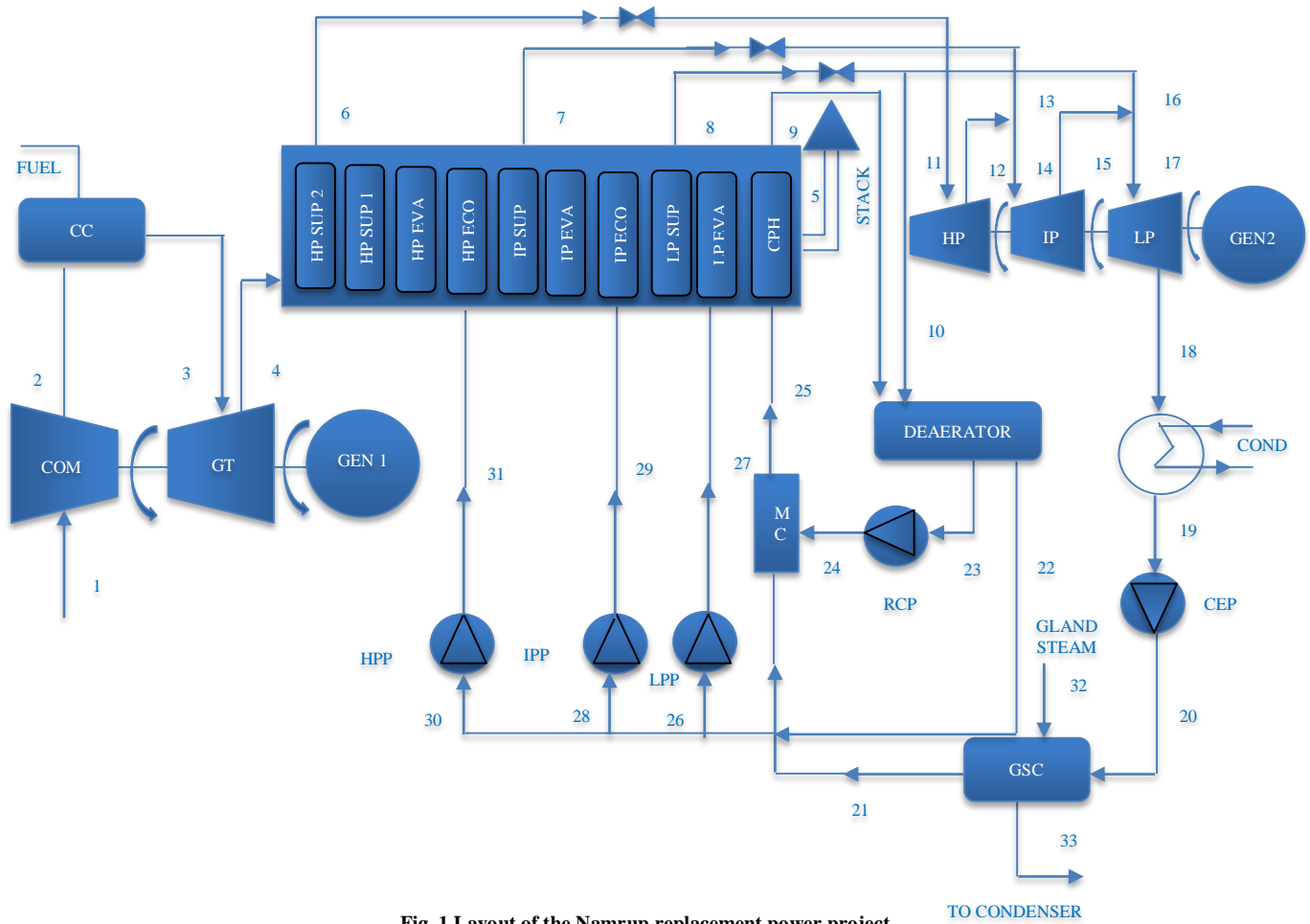


Fig. 1 Layout of the Namrup replacement power project

### 3. Thermodynamic Modeling

A thermodynamic model has been created in this study to predict the system components' energy and exergy performance. Each control volume component is subjected to the mass, energy, and energy balance principle at a steady state. Engineering Equation Solver (EES) software is employed to analyze the complete cycle through the

development of a numerical code based on the model. When modeling the components, the following presumptions were made:

- A steady flow condition is considered for all the components.
- Air and gas mixtures are both considered instances of an ideal gas mixture.

- It is assumed that there will be a 3% pressure drop in the CC.
- There is very little heat released into the environment from the system.

### 3.1. Energy Analysis

Three methods exist for transferring energy to or from an open system: heat transfer, work transfer, and mass transfer or mass flow.

Under steady-state circumstances, the equation for the mass and energy balance of a control volume is provided by Equations (1) and (2), respectively, while ignoring changes in kinetic as well as potential energy.

$$\sum \dot{m}_i = \sum \dot{m}_o \quad (1)$$

$$\dot{Q} + \sum \dot{m}_i h_i = \sum \dot{m}_e h_e + \dot{W} \quad (2)$$

Where the control volume's input and output streams are denoted by i and o, these formulas allow for the analysis of energy interactions among various power plant components, as well as the determination of energy loss and first-law efficiency. The following formula might be employed to determine the CCPP efficiency.

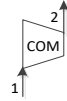
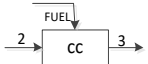
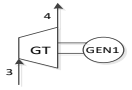
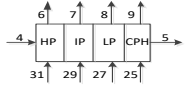
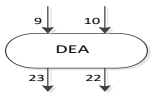
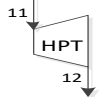
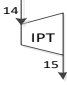
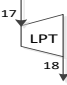
$$\eta_{I,cycle} = \frac{W_{net}}{\dot{m}_f \times LCV} \quad (3)$$

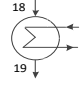
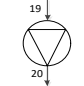
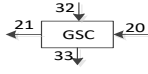

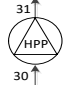
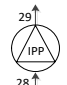
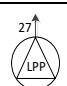
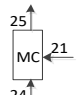
Where,  $W_{net}$ ,  $\dot{m}_f$  LCV is the net power developed, the mass of fuel, and the lower calorific value of fuel accordingly. The cycle efficiency can be computed as follows.

$$\eta_{I,cycle} = 1 - \frac{E_l}{\dot{m}_f \times LCV} \quad (4)$$

Where,  $E_l$  is the energy loss in the component. The energy balance, energy loss, along energy efficiency equations of the components are given in Table 1.

Table 1. Energy balance, energy loss, and energy efficiency equations for the components

| Components         | Energy Balance Equation   | Energy Loss   | Energy Efficiency  | Energy Balance Diagram  |
|--------------------|---|---|--|---|
| Compressor         | $-W_C = \dot{m}_1(h_1 - h_{2s}) - E_{l,C}$  | $E_{l,C} = \dot{m}_1(h_1 - h_{2s}) + W_C$   | $\eta_{l,C} = 1 - \frac{E_{l,C}}{W_C}$                                     |   |
| Combustion Chamber | $\dot{m}_f \times CV = \dot{m}_3 h_3 - \dot{m}_2 h_2 + E_{l,CC}$  | $E_{l,CC} = \dot{m}_f \times CV + (\dot{m}_2 h_2 - \dot{m}_3 h_3)$  | $\eta_{l,CC} = 1 - \frac{E_{l,CC}}{\dot{m}_f \times CV}$                   |  |
| Gas Turbine        | $W_{GT} = \dot{m}_3(h_3 - h_{4s}) - E_{l,GT}$   | $E_{l,GT} = \dot{m}_3(h_3 - h_{4s}) - W_{GT}$   | $\eta_{l,GT} = 1 - \frac{E_{l,GT}}{\dot{m}_3(h_3 - h_{4s})}$               |  |
| HRSG               | $0 = \dot{m}_4(h_4 - h_5) - \dot{m}_6(h_6 - h_{31}) - \dot{m}_7(h_7 - h_{29}) - \dot{m}_8(h_8 - h_{27}) - \dot{m}_9(h_9 - h_{25}) - E_{l,HRSG}$ | $E_{l,HRSG} = \dot{m}_4(h_4 - h_5) - \dot{m}_6(h_6 - h_{31}) - \dot{m}_7(h_7 - h_{29}) - \dot{m}_8(h_8 - h_{27}) - \dot{m}_9(h_9 - h_{25})$ | $\eta_{l,HRSG} = 1 - \frac{E_{l,HRSG}}{\dot{m}_4(h_4 - h_5)}$              |  |
| Deaerator          | $0 = \dot{m}_9 h_9 + \dot{m}_{10} h_{10} - \dot{m}_{22} h_{22} - \dot{m}_{23} h_{23} - E_{l,DEA}$   | $E_{l,DEA} = \dot{m}_9 h_9 + \dot{m}_{10} h_{10} - \dot{m}_{22} h_{22} - \dot{m}_{23} h_{23}$   | $\eta_{l,DEA} = 1 - \frac{E_{l,DEA}}{\dot{m}_9 h_9 + \dot{m}_{10} h_{10}}$ |  |
| HPST               | $W_{HPT} = \dot{m}_{11}(h_{11} - h_{12s}) - E_{l,HPT}$  | $E_{l,HPT} = \dot{m}_{11}(h_{11} - h_{12s}) - W_{HPT}$  | $\eta_{l,HPT} = 1 - \frac{E_{l,HPT}}{\dot{m}_{11}(h_{11} - h_{12s})}$      |  |
| IPST               | $W_{IPT} = \dot{m}_{14}(h_{14} - h_{15s}) - E_{l,IPT}$  | $E_{l,IPT} = \dot{m}_{14}(h_{14} - h_{15s}) - W_{IPT}$  | $\eta_{l,IPT} = 1 - \frac{E_{l,IPT}}{\dot{m}_{14}(h_{14} - h_{15s})}$      |  |
| LPST               | $W_{LPT} = \dot{m}_{17}(h_{17} - h_{18s}) - E_{l,LPT}$  | $E_{l,LPT} = \dot{m}_{17}(h_{17} - h_{18s}) - W_{LPT}$  | $\eta_{l,LPT} = 1 - \frac{E_{l,LPT}}{\dot{m}_{17}(h_{17} - h_{18s})}$      |  |

|           |   |   |  |  |
|-----------|---|---|--|--|
| Condenser | $0 = \dot{m}_{18}(h_{18} - h_{19}) - \dot{Q}_K - E_{I,CON}$                   | $E_{I,CON} = \dot{m}_{18}(h_{18} - h_{19}) - \dot{Q}_K$                   | $\eta_{I,CON} = 1 - \frac{E_{I,CON}}{\dot{m}_{18}(h_{18} - h_{19})}$         |   |
| CEP       | $-W_{CEP} = \dot{m}_{19}(h_{19} - h_{20s}) - E_{I,CEP}$                       | $E_{I,CEP} = \dot{m}_{19}(h_{19} - h_{20s}) + W_{CEP}$                    | $\eta_{I,CEP} = 1 - \frac{E_{I,CEP}}{W_{CEP}}$                               |   |
| GSC       | $0 = \dot{m}_{32}(h_{32} - h_{33}) - \dot{Q}_K - E_{I,GSC}$                   | $E_{I,GSC} = \dot{m}_{32}(h_{32} - h_{33}) - \dot{Q}_K$                   | $\eta_{I,GSC} = 1 - \frac{E_{I,GSC}}{\dot{m}_{32}(h_{32} - h_{33})}$         |   |
| RCP       | $-W_{RCP} = \dot{m}_{23}(h_{23} - h_{24s}) - E_{I,RCP}$                       | $E_{I,RCP} = \dot{m}_{23}(h_{23} - h_{24s}) + W_{RCP}$                    | $\eta_{I,RCP} = 1 - \frac{E_{I,RCP}}{W_{RCP}}$                               |   |
| HPP       | $-W_{HPP} = \dot{m}_{30}(h_{30} - h_{31s}) - E_{I,HPP}$                       | $E_{I,HPP} = \dot{m}_{30}(h_{30} - h_{31s}) + W_{HPP}$                    | $\eta_{I,HPP} = 1 - \frac{E_{I,HPP}}{W_{HPP}}$                               |   |
| IPP       | $-W_{IPP} = \dot{m}_{28}(h_{28} - h_{29s}) - E_{I,IPP}$                       | $E_{I,IPP} = \dot{m}_{28}(h_{28} - h_{29s}) + W_{IPP}$                    | $\eta_{I,IPP} = 1 - \frac{E_{I,IPP}}{W_{IPP}}$                               |   |
| LPP       | $-W_{LPP} = \dot{m}_{26}(h_{26} - h_{27s}) - E_{I,LPP}$                       | $E_{I,LPP} = \dot{m}_{26}(h_{26} - h_{27s}) + W_{LPP}$                    | $\eta_{I,LPP} = 1 - \frac{E_{I,LPP}}{W_{LPP}}$                               |   |
| MC        | $0 = \dot{m}_{21}h_{21} + \dot{m}_{24}h_{24} - \dot{m}_{25}h_{25} - E_{I,MC}$ | $E_{I,MC} = \dot{m}_{21}h_{21} + \dot{m}_{24}h_{24} - \dot{m}_{25}h_{25}$ | $\eta_{I,MC} = 1 - \frac{E_{I,MC}}{\dot{m}_{21}h_{21} + \dot{m}_{24}h_{24}}$ |  |

### 3.2. Exergy Analysis

The most valuable work a system can do is when it reaches its ultimate state of equilibrium with its environment. Exergy can be categorized into physical, chemical, kinetic, and potential types. Kinetic and potential exergy are often ignored due to their minimal amount. "Physical exergy" refers to the maximum theoretically achievable work when a system interacts with a reference environment at equilibrium. "Chemical exergy" measures how a system's chemical composition differs from that of its reference environment. The following formula provides the energy balance for a thermal system under steady-state conditions: [1, 27, 29].

$$\dot{X}_Q + \sum \dot{m}_i \psi_i = \sum \dot{m}_o \psi_o + \dot{W} - \dot{I}_d \quad (5)$$

Where,  $\dot{X}_Q$  and  $\dot{W}$  represent the net exergy transferred by heat and useful work done by the system, respectively, while the irreversibility or exergy destruction is represented by  $\dot{I}_d$ . The subscripts i and o refer to the inlet and outlet states. The net exergy transferred by heat  $\dot{Q}$  at the temperature  $T_k$  given by [27-30].

$$\dot{x}_Q = \sum \left( 1 - \frac{T_0}{T_k} \right) \dot{Q} \quad (6)$$

The exergy destruction can be expressed as,

$$\dot{I}_d = T_0 \dot{S}_{gen} \quad (7)$$

Here  $\dot{S}_{gen}$  is the system's entropy generation.

The specific flow exergy is given by

$$\psi = (h - h_0) - T_0 (s - s_0) \quad (8)$$

The total flow exergy is given by

$$\dot{X} = \dot{m} \psi = \dot{m} [(h - h_0) - T_0 (s - s_0)] \quad (9)$$

To determine a gas mixture's chemical exergy, use the following formula [1, 2].

$$ex_{mix}^{ch} = \sum_{i=1}^n x_i ex_i^{ch} + RT_0 \sum_{i=1}^n x_i \ln x_i \quad (10)$$

However, fuel exergy cannot be determined using the equation above. As a result, the following simpler equation is utilized to compute the fuel exergy [21].

$$\xi = \frac{ex_f}{LHV_f} \quad (11)$$

For gaseous fuel having chemical composition  $C_xH_y$  [2, 12]

$$\xi = 1.033 + 0.0169 \frac{y}{x} - \frac{0.0698}{x} \quad (12)$$

Here  $\xi$  is the exergy factor. For natural gas, the exergetic factor can be considered as (1.04±0.5%) [27, 30].

The exergetic efficiency of the CCPP can be computed as follows:

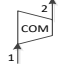
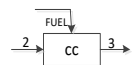
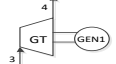


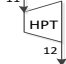
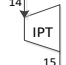
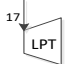
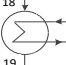


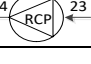
$$\eta_{II,cycle} = \frac{W_{net}}{\xi \times \dot{m}_f \times LCV} \quad (13)$$

The exergetic efficiency of the components is given by,

$$\eta_{II,component} = 1 - \frac{\dot{I}_d}{\xi \times \dot{m}_f \times LCV} \quad (14)$$

Table 2 contains the equations for the exergy balance, exergy destruction, and exergy efficiency of each major component.

Table 2. Exergy balance, exergy destruction, and exergy efficiency equations for the components

| Components         | Exergy Balance Equation   | Exergy Destruction  | Exergy Efficiency  | Exergy Balance Diagram  |
|--------------------|---|---|--|---|
| Compressor         | $-W_C = \dot{m}_1(\psi_1 - \psi_{2s}) - \dot{I}_{d,C}$  | $\dot{I}_{d,C} = \dot{m}_1(\psi_1 - \psi_{2s}) + W_C$   | $\eta_{II,C} = 1 - \frac{\dot{I}_{d,C}}{W_C}$  |    |
| Combustion Chamber | $0 = \dot{m}_2\psi_2 + \dot{m}_f\psi_f - \dot{m}_3\psi_3 - \dot{I}_{d,CC}$  | $\dot{I}_{d,CC} = \dot{m}_2\psi_2 + \dot{m}_f\psi_f - \dot{m}_3\psi_3$  | $\eta_{II,CC} = 1 - \frac{\dot{I}_{d,CC}}{\dot{m}_2\psi_2 + \dot{m}_f\psi_f}$                |    |
| Gas Turbine        | $W_{GT} = \dot{m}_3(\psi_3 - \psi_{4s}) - \dot{I}_{d,GT}$   | $\dot{I}_{d,GT} = \dot{m}_3(\psi_3 - \psi_{4s}) - W_{GT}$   | $\eta_{II,GT} = 1 - \frac{\dot{I}_{d,GT}}{\dot{m}_3(\psi_3 - \psi_4)}$                       |    |
| HRSG               | $0 = \dot{m}_4(\psi_4 - \psi_5) - \dot{m}_6(\psi_6 - \psi_{31}) - \dot{m}_7(\psi_7 - \psi_{29}) - \dot{m}_8(\psi_8 - \psi_{27}) - \dot{m}_9(\psi_9 - \psi_{25}) - \dot{I}_{d,HRSG}$ | $\dot{I}_{d,HRSG} = \dot{m}_4(\psi_4 - \psi_5) - \dot{m}_6(\psi_6 - \psi_{31}) - \dot{m}_7(\psi_7 - \psi_{29}) - \dot{m}_8(\psi_8 - \psi_{27}) - \dot{m}_9(\psi_9 - \psi_{25})$ | $\eta_{II,HRSG} = 1 - \frac{\dot{I}_{d,HRSG}}{\dot{m}_4(\psi_4 - \psi_5)}$                   |    |
| Deaerator          | $0 = \dot{m}_9\psi_9 + \dot{m}_{10}\psi_{10} - \dot{m}_{22}\psi_{22} - \dot{m}_{23}\psi_{23} - \dot{I}_{d,DEA}$   | $\dot{I}_{d,DEA} = \dot{m}_9\psi_9 + \dot{m}_{10}\psi_{10} - \dot{m}_{22}\psi_{22} - \dot{m}_{23}\psi_{23}$   | $\eta_{II,DEA} = 1 - \frac{\dot{I}_{d,DEA}}{\dot{m}_9\psi_9 + \dot{m}_{10}\psi_{10}}$        |  |
| HPST               | $W_{HPT} = \dot{m}_{11}\psi_{11} - \dot{m}_{12}\psi_{12S} - \dot{I}_{d,HPT}$  | $\dot{I}_{d,HPT} = \dot{m}_{11}\psi_{11} - \dot{m}_{12}\psi_{12S} - W_{HPT}$  | $\eta_{II,HPT} = 1 - \frac{\dot{I}_{d,HPT}}{\dot{m}_{11}\psi_{11} - \dot{m}_{12}\psi_{12S}}$ |  |
| IPST               | $W_{IPT} = \dot{m}_{14}\psi_{14} - \dot{m}_{15}\psi_{15S} - \dot{I}_{d,IPT}$  | $\dot{I}_{d,IPT} = \dot{m}_{14}\psi_{14} - \dot{m}_{15}\psi_{15S} - W_{IPT}$  | $\eta_{II,IPT} = 1 - \frac{\dot{I}_{d,IPT}}{\dot{m}_{14}\psi_{14} - \dot{m}_{15}\psi_{15S}}$ |  |
| LPST               | $W_{LPT} = \dot{m}_{17}\psi_{17} - \dot{m}_{18}\psi_{18S} - \dot{I}_{d,LPT}$  | $\dot{I}_{d,LPT} = \dot{m}_{17}\psi_{17} - \dot{m}_{18}\psi_{18S} - W_{LPT}$  | $\eta_{II,LPT} = 1 - \frac{\dot{I}_{d,LPT}}{\dot{m}_{17}\psi_{17} - \dot{m}_{18}\psi_{18S}}$ |  |
| Condenser          | $0 = \dot{m}_{18}(\psi_{18} - \psi_{19}) - \left(1 - \frac{T_0}{T_k}\right) \dot{Q} - \dot{I}_{d,CON}$  | $\dot{I}_{d,CON} = \dot{m}_{18}(\psi_{18} - \psi_{19}) - \left(1 - \frac{T_0}{T_k}\right) \dot{Q}$  | $\eta_{II,CON} = 1 - \frac{\dot{I}_{d,CON}}{\dot{m}_{18}(\psi_{18} - \psi_{19})}$            |  |
| CEP                | $-W_{CEP} = \dot{m}_{19}(\psi_{19} - \psi_{20S}) - \dot{I}_{d,CEP}$   | $\dot{I}_{d,CEP} = \dot{m}_{19}(\psi_{19} - \psi_{20S}) + W_{CEP}$  | $\eta_{II,CEP} = 1 - \frac{\dot{I}_{d,CEP}}{W_{CEP}}$  |  |
| GSC                | $0 = \dot{m}_{32}(\psi_{32} - \psi_{33}) - \left(1 - \frac{T_0}{T_k}\right) \dot{Q} - \dot{I}_{d,GSC}$  | $\dot{I}_{d,GSC} = \dot{m}_{32}(\psi_{32} - \psi_{33}) - \left(1 - \frac{T_0}{T_k}\right) \dot{Q}_k$  | $\eta_{II,GSC} = 1 - \frac{\dot{I}_{d,GSC}}{\dot{m}_{32}(\psi_{32} - \psi_{33})}$            |  |
| RCP                | $-W_{RCP} = \dot{m}_{23}(\psi_{23} - \psi_{24s}) - \dot{I}_{d,RCP}$   | $\dot{I}_{d,RCP} = \dot{m}_{23}(\psi_{23} - \psi_{24}) + W_{RCP}$   | $\eta_{II,RCP} = 1 - \frac{\dot{I}_{d,RCP}}{W_{RCP}}$  |  |

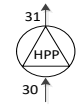
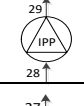
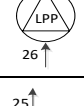
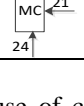
|     |  |  |   |   |
|-----|--|--|---|---|
| HPP | $-W_{HPP} = \dot{m}_{30}(\psi_{30} - \psi_{31S}) - \dot{I}_{d,HPP}$                          | $\dot{I}_{d,HPP} = \dot{m}_{30}(\psi_{30} - \psi_{31S}) + W_{HPP}$                       | $\eta_{II,HPP} = 1 - \frac{\dot{I}_{d,HPP}}{W_{HPP}}$                                     |  |
| IPP | $-W_{IPP} = \dot{m}_{28}(\psi_{28} - \psi_{29S}) - \dot{I}_{d,IPP}$                          | $\dot{I}_{d,IPP} = \dot{m}_{28}(\psi_{28} - \psi_{29S}) + W_{IPP}$                       | $\eta_{II,IPP} = 1 - \frac{\dot{I}_{d,IPP}}{W_{IPP}}$                                     |  |
| LPP | $-W_{LPP} = \dot{m}_{26}(\psi_{26} - \psi_{27S}) - \dot{I}_{d,LPP}$                          | $\dot{I}_{d,LPP} = \dot{m}_{26}(\psi_{26} - \psi_{27S}) + W_{LPP}$                       | $\eta_{II,LPP} = 1 - \frac{\dot{I}_{d,LPP}}{W_{LPP}}$                                     |  |
| MC  | $O = \dot{m}_{21}\psi_{21} + \dot{m}_{24}\psi_{24} - \dot{m}_{25}\psi_{25} - \dot{I}_{d,MC}$ | $\dot{I}_{d,MC} = \dot{m}_{21}\psi_{21} + \dot{m}_{24}\psi_{24} - \dot{m}_{25}\psi_{25}$ | $\eta_{II,MC} = 1 - \frac{\dot{I}_{d,MC}}{\dot{m}_{21}\psi_{21} + \dot{m}_{24}\psi_{24}}$ |  |

Table 3. Operating parameters of the CCPP

| Component                 | Operating Parameters |
|---------------------------|----------------------|
| Ambient Temperature       | 306 K                |
| Ambient Pressure          | 1.0123 bar           |
| Air Flow Rate             | 154.85 kg/s          |
| Fuel Flow Rate            | 4.043 kg/s           |
| Compression Ratio         | 12.72                |
| Turbine Inlet Temperature | 1528 K               |
| Turbine Exit Temperature  | 896 K                |
| LCV of Fuel               | 46547 kJ/kg          |
| Exergy Factor             | 1.04                 |

#### 4. Results and Discussion

The investigation of the natural gas-fired combined cycle’s performance takes into account various operating parameters, including mass flow, pressure, as well as temperature for every component. At the compressor inlet, the inlet air conditions are set to 1.0123 bar and 306 K. The operating parameters, which are collected from the plant control room, are presented in Table 3. During the operation,

92.5 MW of net power was developed. Because of certain assumptions were taken into consideration, the net power that our developed model yielded was 92.677 MW, which is somewhat higher. The gas cycle and steam cycle have respective efficiencies of 32.98%, 31.72%, and 32.04%, 30.80%, while the CCPP has an energetic and exergetic efficiency of 49.24% and 47.25%. Table 4 displays the results of the computation of the thermodynamic characteristics of each state point using the EES code.

Table 5 displays the energy and exergy performance of every component under operating conditions. Figure 2 displays the energy and exergy efficiency of the various plant components. It has been observed that the condenser experiences the greatest energy loss, accounting for about 35.72% of the total energy supplied. This is caused by equipment loss as well as the rejection of heat to the cooling water during the phase transition from wet steam to water. Of the total energy supplied, the energy lost in the gas turbine, compressor, and HRSG is 6.87%, 2.75%, and 0.86%, respectively and 5.99% of the energy is lost to the atmosphere via the stack.

Table 4. Properties of thermodynamics at state points

| 02State | P (bar) | T (K) | $\dot{m}$ (kg/s) | h (kJ/kg.K) | s (kJ/kg.K) | $\psi$ (kJ/kg.K) | $\dot{X}$ (kW) |
|---------|---------|-------|------------------|-------------|-------------|------------------|----------------|
| 1       | 1.013   | 306   | 154.85           | 306.50      | 5.722       | 0                | 0              |
| 2       | 12.72   | 662   | 154.85           | 673         | 5.786       | 346.70           | 53686.50       |
| 3       | 12.34   | 1528  | 158.89           | 1808        | 6.891       | 1088             | 172872.30      |
| 4       | 1.04    | 896   | 158.89           | 1060        | 6.985       | 311.50           | 49494.24       |
| 5       | 1.013   | 366   | 158.89           | 433.10      | 5.934       | 6.165            | 979.5569       |
| 6       | 76.49   | 813   | 27.30            | 3501        | 6.874       | 1405             | 38356.50       |
| 7       | 22.94   | 533   | 2.11             | 2916        | 6.514       | 930.30           | 1962.933       |
| 8       | 4.60    | 470   | 1.30             | 2851        | 7.089       | 689.80           | 896.74         |
| 9       | 2.942   | 373   | 42.51            | 418.70      | 1.305       | 27.10            | 1152.021       |
| 10      | 4.462   | 473   | 0.383            | 2858        | 7.117       | 688.10           | 263.5423       |
| 11      | 74.20   | 813   | 27.22            | 3503        | 6.89        | 1402             | 38162.44       |



|    |       |        |       |        |        |        |          |
|----|-------|--------|-------|--------|--------|--------|----------|
| 12 | 22.25 | 650    | 27.22 | 3193   | 6.998  | 1059   | 28825.98 |
| 13 | 22.25 | 533    | 2.11  | 2919   | 6.532  | 927.60 | 1957.236 |
| 14 | 22.25 | 641.20 | 29.33 | 3173   | 6.967  | 1049   | 30767.17 |
| 15 | 4.462 | 470    | 29.33 | 2852   | 7.104  | 685.90 | 20117.45 |
| 16 | 4.462 | 470    | 0.916 | 2852   | 7.104  | 685.90 | 628.2844 |
| 17 | 4.462 | 470    | 30.25 | 2852   | 7.104  | 685.90 | 20748.48 |
| 18 | 0.125 | 323.40 | 30.25 | 2431   | 7.574  | 121.4  | 3672.35  |
| 19 | 0.125 | 323    | 30.33 | 208.70 | 0.7019 | 1.815  | 55.04895 |
| 20 | 7.845 | 323.20 | 30.71 | 210    | 0.7035 | 2.624  | 80.58304 |
| 21 | 7.626 | 324    | 30.33 | 213.50 | 0.7144 | 2.795  | 84.77235 |
| 22 | 1.128 | 376    | 30.71 | 431.20 | 1.339  | 29.23  | 897.6533 |
| 23 | 1.128 | 376    | 12.18 | 431.20 | 1.339  | 29.23  | 356.0214 |
| 24 | 6.86  | 376.10 | 12.18 | 432    | 1.34   | 29.88  | 363.9384 |
| 25 | 6.86  | 338    | 42.51 | 272    | 0.8914 | 7.131  | 303.1388 |
| 26 | 1.128 | 376    | 1.30  | 431.20 | 1.339  | 29.23  | 37.999   |
| 27 | 8.75  | 376.20 | 1.30  | 432.40 | 1.34   | 30.11  | 39.143   |
| 28 | 1.128 | 376    | 2.11  | 431.20 | 1.339  | 29.23  | 61.6753  |
| 29 | 27.45 | 376.50 | 2.11  | 435.30 | 1.343  | 32.23  | 68.0053  |
| 30 | 1.128 | 376    | 27.30 | 431.20 | 1.339  | 29.23  | 797.979  |
| 31 | 84.32 | 377.70 | 27.30 | 444.50 | 1.352  | 38.80  | 1059.24  |
| 32 | 0.25  | 530    | 0.08  | 2990   | 8.704  | 335.10 | 26.808   |
| 33 | 0.25  | 338    | 0.08  | 271.50 | 0.8918 | 6.439  | 0.51512  |

Table 5. Performance results of cycle components of the NRPP

| SL. No.         | Components | Energy Loss (kW) | % Ratio | Energy Efficiency | Exergy Loss (kW) | % Ratio | Exergy Efficiency |
|-----------------|------------|------------------|---------|-------------------|------------------|---------|-------------------|
| 1               | COM        | 5186             | 2.756   | 90.86             | 3062             | 1.565   | 94.6              |
| 2               | CC         | 1328             | 0.706   | 99.29             | 72564            | 37.076  | 62.17             |
| 3               | GT         | 12945            | 6.879   | 90.18             | 8345             | 4.264   | 93.67             |
| 4               | HRSRG      | 1631             | 0.867   | 98.36             | 7613             | 3.890   | 69.46             |
| 5               | DEA        | 398.30           | 0.212   | 97.89             | 161.70           | 0.083   | 88.58             |
| 6               | HPST       | 1857             | 0.987   | 81.97             | 895.20           | 0.457   | 90.41             |
| 7               | IPST       | 1824             | 0.969   | 83.78             | 1253             | 0.640   | 88.27             |
| 8               | LPST       | 4621             | 2.456   | 73.32             | 4372             | 2.234   | 74.39             |
| 9               | COND       | 67221            | 35.72   | 48.10             | 2894             | 1.479   | 26.91             |
| 10              | CEP        | 15.52            | 0.008   | 60.42             | 14.66            | 0.007   | 62.52             |
| 11              | GSC        | 110.30           | 0.059   | 49.28             | 11.19            | 0.006   | 57.45             |
| 12              | RCP        | 3.04             | 0.002   | 70.62             | 2.47             | 0.001   | 76.09             |
| 13              | HPP        | 127.50           | 0.068   | 65.03             | 103.40           | 0.053   | 71.63             |
| 14              | IPP        | 2.78             | 0.001   | 67.60             | 2.26             | 0.001   | 73.66             |
| 15              | LPP        | 0.52             | 0.000   | 66.37             | 0.43             | 0.001   | 72.64             |
| 16              | MC         | 173.80           | 0.092   | 98.52             | 145.50           | 0.074   | 67.56             |
| 17              | STACK      | 11281            | 5.994   |                   | 1849             | 0.945   | 11281             |
| Energy Supplied |            | 188189.52        |         | Exergy Supplied   | 195717.10        |         |                   |

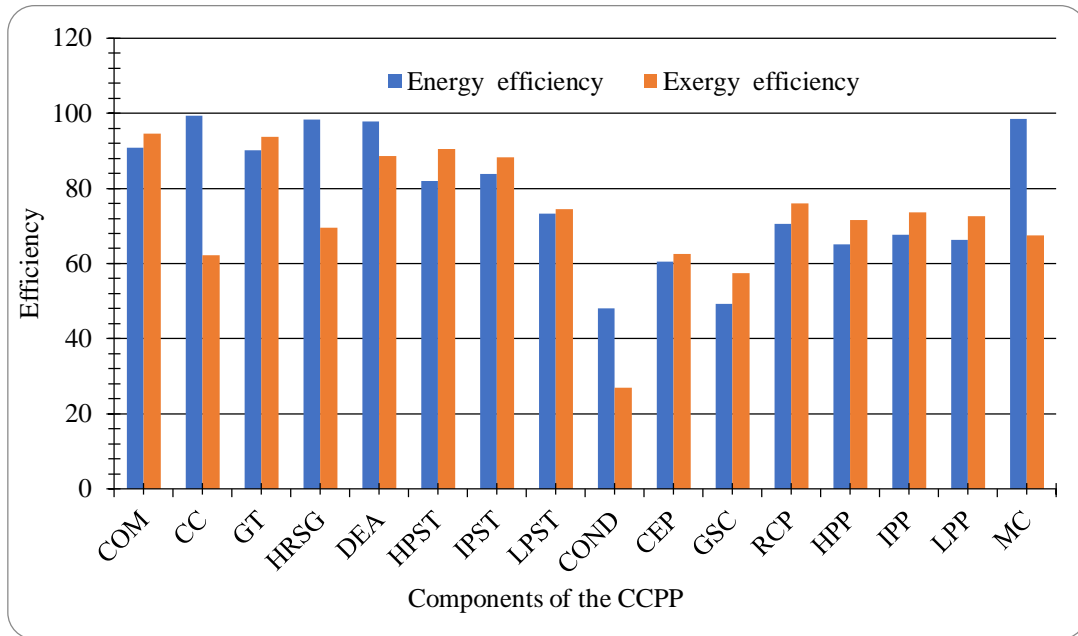


Fig. 2 Energy and exergy efficiency of cycle components

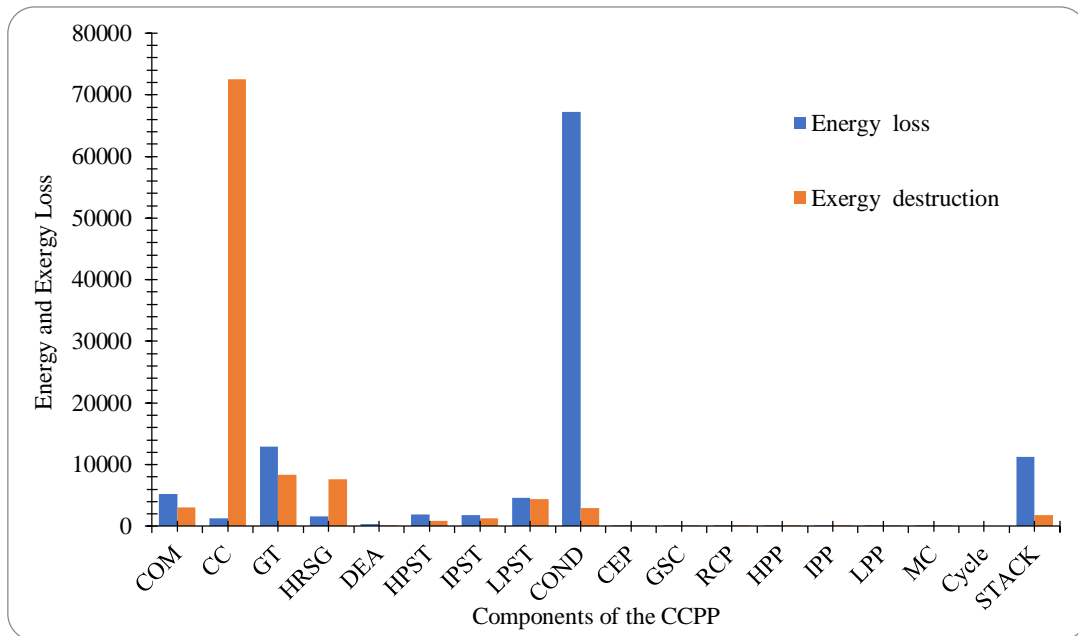


Fig. 3 Energy and exergy destruction of cycle components

Figure 3 depicts the exergy destruction of every component. The exergy investigation shows that chemical interactions and the temperature difference between the working fluid and the burners cause the most exergy loss in the combustion chamber. Combustion chamber exergy destruction is 72.564 MW, higher than other components. Higher irreversibility reduces exergy efficiency. The gas turbine (4.26%) had the second-highest exergy destruction, with the steam turbine (3.33%) and HRSG (3.89%) coming

next. Compressor exergy loss changes with compression ratio and turbine inlet temperature, as seen in Figure 4. As the compression ratio increases at a fixed turbine inlet temperature, compressor exergy loss decreases. This is because as the compression ratio increases, compressor efficiency also increases. Exergy destruction decreases gradually as the compression ratio rises at low turbine inlet temperatures, but it decreases quickly at higher turbine inlet temperatures.

Figure 5 shows how compression ratio and turbine inlet temperature affect combustion chamber exergy loss. As the compression ratio increases, combustion chamber exergy loss decreases at a given turbine inlet temperature. Increased turbine inlet temperature improves combustion chamber efficiency. This reduces energy destruction. Exergy destruction in the combustion chamber decreases gradually as the compression ratio increases at low turbine inlet temperatures, but it decreases quickly at higher turbine inlet temperatures.

Figure 6 illustrates how the gas turbine's exergy loss changes as the compression ratio and turbine inlet temperature change. It has been noted that the exergy loss is greater at low turbine inlet temperatures and rapidly decreases with

increasing turbine inlet temperature. At any given turbine inlet temperature, the exergy loss increases as the compression ratio increases.

Figures 7 and 8 illustrate how the ambient temperature affects the combined cycle power plant's net power output and exergetic efficiency. The system's performance is adversely affected by rising ambient temperature because it causes the compressor to use more power and causes energy loss.

The density of the air decreases with elevating temperature, elevating the compressor's power consumption and lowering net power. Since net power output and exergetic efficiency are inversely connected with ambient temperature, they exhibit a similar trend as ambient temperature changes.

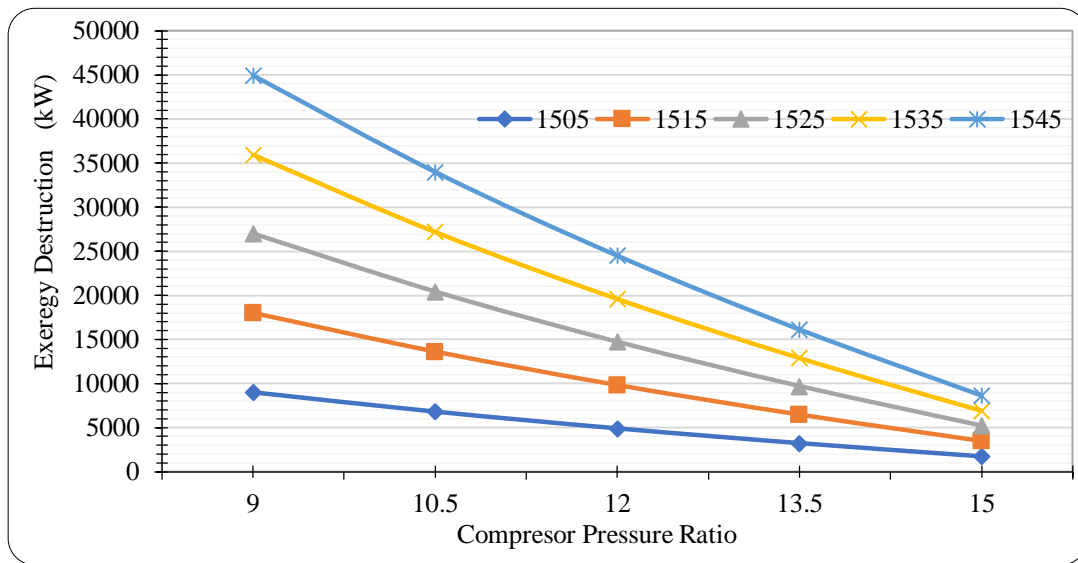


Fig. 4 Effect of turbine inlet temperature and pressure ratio on exergy destruction in compressor

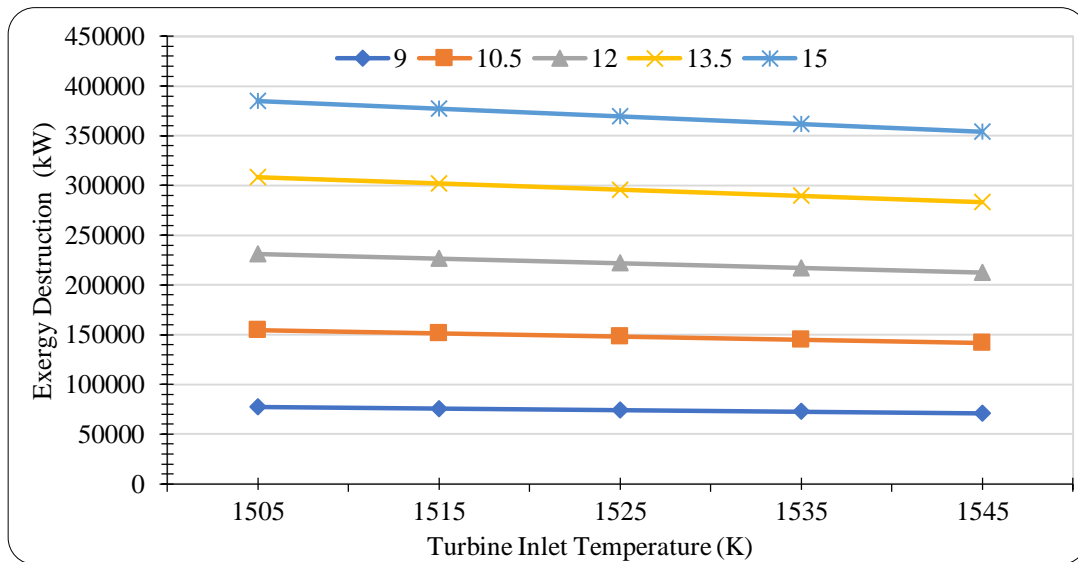


Fig. 5 Effect of turbine inlet temperature and pressure ratio on exergy destruction in combustion

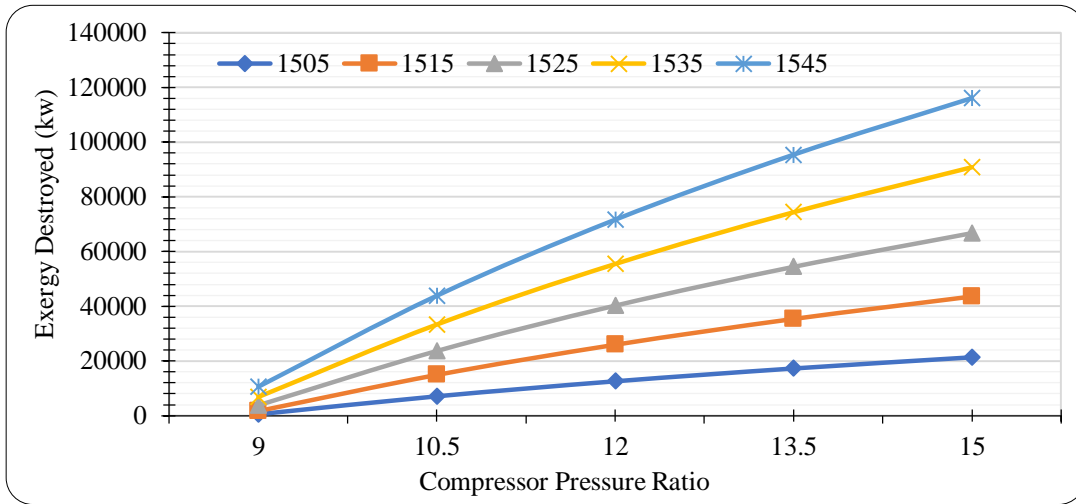


Fig. 6 Effect and turbine inlet temperature and pressure ratio on exergy destruction in gas turbine

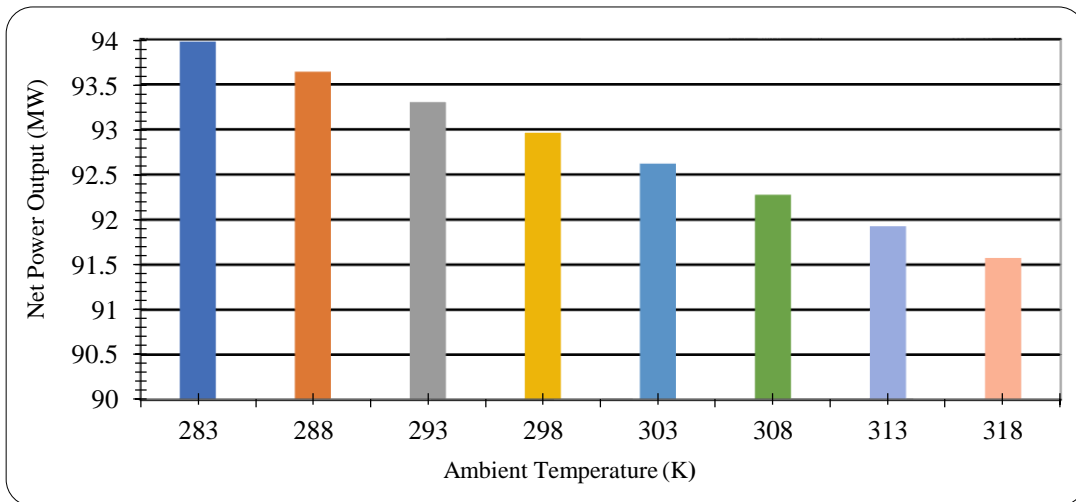


Fig. 7 Effect of ambient temperature on the net power output

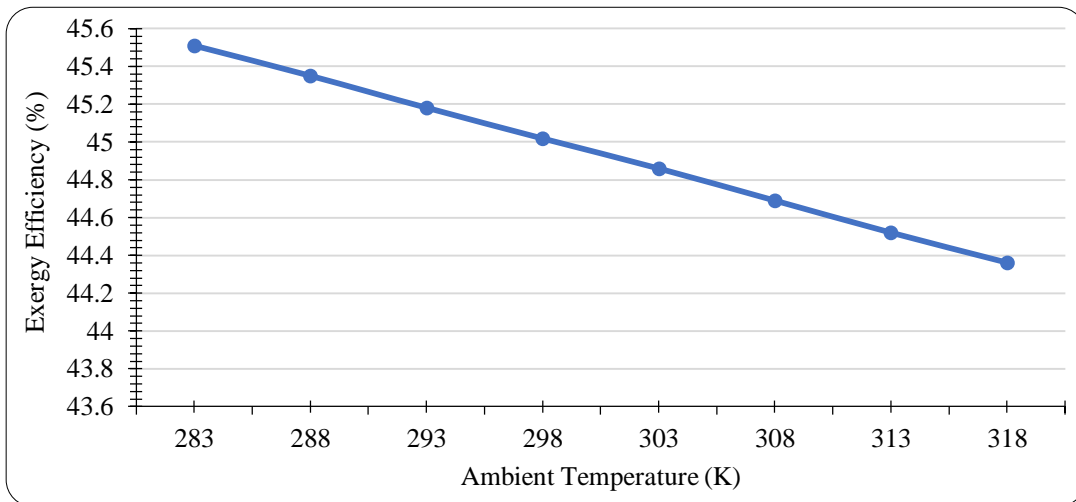


Fig. 8 Effect of ambient temperature on exergy efficiency

## 5. Conclusion

In this research, energy as well as exergy analysis using operating data is employed to investigate the performance of all the components of NRPP. The following lists are the primary findings from this analysis.

- The combined cycle power plant has an efficiency of 47.25 percent for exergy and 49.24 percent for l energy.
- The condenser is the cycle's main energy destructor, as per the energy results.
- The combustion chamber is the most irreversible component, followed by the steam turbine, gas turbine, and HRSG.
- The compressor, combustion chamber, and gas turbine all experience different levels of exergy destruction depending on the compression ratio and gas turbine inlet temperature.
- The net output of the cycle is decreased with a rise in ambient temperature.

The combustors require special attention, and methods for lowering this irreversibility should be devised to raise the plant's power "output.

## Contribution of Authors

B. K. Roy: Conceived design research, data collection, development of the thermodynamics model, analysis, writing, reviewing, R. Sharma: Conceived design research, analysis and reviewing and D. K. Rabha. Conceived design research, data collection, analysis, writing, reviewing.

## Nomenclature

### Symbols

|           |                            |
|-----------|----------------------------|
| T         | Temperature (K)            |
| P         | Pressure (bar)             |
| $\dot{m}$ | Mass Flow Rate (kg/s)      |
| Q         | Rate of Heat Transfer (kW) |
| W         | Power (kW)                 |

|               |                                     |
|---------------|-------------------------------------|
| h             | Specific Enthalpy (kJ/kg)           |
| s             | Specific Entropy (kJ/kg.K)          |
| cpa           | Specific Heat of Air (kJ/kg.K)      |
| cpg           | Specific Heat of Gas (kJ/kg.K)      |
| $\dot{X}$     | Total Exergy Rate (kW)              |
| LCV           | Lower Calorific Value (kJ/kg)       |
| Abbreviations |                                     |
| CCPP          | Combined Cycle Power Plant          |
| NTPS          | Namrup Thermal Power Station        |
| NRPP          | Namrup Replacement Power Project    |
| C             | Compressor                          |
| CC            | Combustion Chamber                  |
| GT            | Gas Turbine                         |
| HRSG          | Heat Recovery Steam Generator       |
| DEA           | Deaerator                           |
| HPST          | High Pressure Steam Turbine         |
| IPST          | Intermediate Pressure Steam Turbine |
| LPST          | Low Pressure Steam Turbine          |
| COND          | Condenser                           |
| CEP           | Condensate Extraction Pump          |
| RCP           | Re-Circulating Pump                 |
| HPP           | High Pressure Pump                  |
| IPP           | Intermediate Pressure Pump          |
| LPP           | Low Pressure Pump                   |
| TIT           | Turbine Inlet Temperature           |
| MC            | Mixing Chamber                      |
| Greek symbols |                                     |
| $\eta_I$      | Energy Efficiency                   |
| $\eta_{II}$   | Exergy Efficiency                   |
| $\Psi$        | Specific Exergy (kJ/Kg)             |

### Exergy factor

#### Subscripts

|   |                   |
|---|-------------------|
| i | Inlet             |
| o | Outlet            |
| 0 | Ambient condition |
| f | Fuel              |
| d | Destruction       |
| l | Loss              |

## References

- [1] Ibrahim Dincer, and Yunus A. Cengel, "Energy, Entropy and Exergy Concepts and Their Roles in Thermal Engineering," *Entropy*, vol. 3, no. 3, pp. 116-149, 2001. [[CrossRef](#)] [[Google Scholar](#)] [[Publisher Link](#)]
- [2] Pouria Ahmadi, Ibrahim Dincer, and Marc A. Rosen, "Exergy, Exergoeconomic and Environmental Analyses and Evolutionary Algorithm Based Multi-Objective Optimization of Combined Cycle Power Plants," *Energy*, vol. 36, no. 10, pp. 5886-5898, 2011. [[CrossRef](#)] [[Google Scholar](#)] [[Publisher Link](#)]
- [3] M.A. Ehyaei, A. Mozafari, and M.H. Alibiglou, "Exergy, Economic & Environmental (3E) Analysis of Inlet Fogging for Gas Turbine Power Plant," *Energy*, vol. 36, no. 12, pp. 6851-6861, 2011. [[CrossRef](#)] [[Google Scholar](#)] [[Publisher Link](#)]
- [4] Saziye Balku, "Analysis of Combined Cycle Efficiency by Simulation and Optimization," *Energy Conversion and Management*, vol. 148, pp. 174-183, 2017. [[CrossRef](#)] [[Google Scholar](#)] [[Publisher Link](#)]
- [5] Sina Kazemi Bakhshmand et al., "Exergoeconomic Analysis and Optimization of a Triple-Pressure Combined Cycle Plant Using Evolutionary Algorithm," *Energy*, vol. 93, pp. 555-567, 2015. [[CrossRef](#)] [[Google Scholar](#)] [[Publisher Link](#)]
- [6] Amin Mohammadi Khoshkar Vandani, Fatemeh Joda, and Ramin Bozorgmehry Boozarjomehry, "Exergic, Economic and Environmental Impacts of Natural Gas and Diesel in Operation of Combined Cycle Power Plants," *Energy Conversion and Management*, vol. 109, pp. 103-112, 2016. [[CrossRef](#)] [[Google Scholar](#)] [[Publisher Link](#)]

- [7] Thamir K. Ibrahim, M.M. Rahman, and Ahmed N. Abdalla, "Gas Turbine Configuration for Improving the Performance of Combined Cycle Power Plant," *Procedia Engineering*, vol. 15, pp. 4216-4223, 2011. [[CrossRef](#)] [[Google Scholar](#)] [[Publisher Link](#)]
- [8] Fateme Ahmadi Boyaghchi, and Hanieh Molaie, "Investigating the Effect of Duct Burner Fuel Mass Flow Rate on Exergy Destruction of a Real Combined Cycle Power Plant Components Based on Advanced Exergy Analysis," *Energy Conversion and Management*, vol. 103, pp. 827–835, 2015. [[CrossRef](#)] [[Google Scholar](#)] [[Publisher Link](#)]
- [9] T.K. Gogoi, and K. Talukdar, "Exergy Based Parametric Analysis of a Combined Reheat Regenerative Thermal Power Plant and Water–LiBr Vapor Absorption Refrigeration System," *Energy Conversion and Management*, vol. 83, pp. 119-132, 2014. [[CrossRef](#)] [[Google Scholar](#)] [[Publisher Link](#)]
- [10] Lava Talib Shireef, and Thamir K. Ibrahim, "Influence of Operating Parameters on the Performance of Combined Cycle Based on Exergy Analysis," *Case Studies in Thermal Engineering*, vol. 40, pp. 1-17, 2022. [[CrossRef](#)] [[Google Scholar](#)] [[Publisher Link](#)]
- [11] Sairam Adibhatla, and S.C. Kaushik, "Energy and Exergy Analysis of a Super Critical Thermal Power Plant at Various Load Conditions Under Constant and Pure Sliding Pressure Operation," *Applied Thermal Engineering*, vol. 73, no. 1, pp. 51-65, 2014. [[CrossRef](#)] [[Google Scholar](#)] [[Publisher Link](#)]
- [12] M. Ameri, P. Ahmadi, and S. Khanmohammad, "Exergy Analysis of a 420MW Combined Cycle Power Plant," *International Journal of Energy Research*, vol. 32, no. 2, pp. 175-183, 2008. [[CrossRef](#)] [[Google Scholar](#)] [[Publisher Link](#)]
- [13] Ahmet Cihann, Oktay Hacıhafızoglu, and Kamil Kahveci, "Energy–Exergy Analysis and Modernization Suggestions for a Combined-Cycle Power Plant," *International Journal of Energy Research*, vol. 30, no. 2, pp. 115-126, 2006. [[CrossRef](#)] [[Google Scholar](#)] [[Publisher Link](#)]
- [14] Omar J. Khaleel et al., "Developing an Analytical Model to Predict the Energy and Exergy Based Performances of a Coal-Fired Thermal Power Plant," *Case Studies in Thermal Engineering*, vol. 28, pp. 1-20, 2021. [[CrossRef](#)] [[Google Scholar](#)] [[Publisher Link](#)]
- [15] Mansur Aliyu et al., "Energy, Exergy and Parametric Analysis of a Combined Cycle Power Plant," *Thermal Science and Engineering Progress*, vol. 15, 2020. [[CrossRef](#)] [[Google Scholar](#)] [[Publisher Link](#)]
- [16] Arvind Tiwari, M. Hasan, and Mohd. Islam, "Exergy Analysis of Combined Cycle Power Plant: NTPC Dadri, India," *International Journal of Thermodynamics*, vol. 16, no. 1, pp. 36-42, 2013. [[Google Scholar](#)] [[Publisher Link](#)]
- [17] A.A.A. Abuelnuor et al., "Exergy Analysis of Garri "2" 180MW Combined Cycle Power Plant," *Renewable and Sustainable Energy Reviews*, vol. 79, pp. 960–969, 2017. [[CrossRef](#)] [[Google Scholar](#)] [[Publisher Link](#)]
- [18] Erdem Ersayin, and Leyla Ozgener, "Performance Analysis of Combined Cycle Power Plants: A Case Study," *Renewable and Sustainable Energy Reviews*, vol. 43, pp. 832–842, 2015. [[CrossRef](#)] [[Google Scholar](#)] [[Publisher Link](#)]
- [19] Isam H. Aljundi, "Energy and Exergy Analysis of a Steam Power Plant in Jordan," *Applied Thermal Engineering*, vol. 29, no. 2-3, pp. 324–328, 2009. [[CrossRef](#)] [[Google Scholar](#)] [[Publisher Link](#)]
- [20] S. Sengupta, A. Datta, and S. Duttgupta, "Exergy Analysis of a Coal-Based 210MW Thermal Power Plant," *International Journal of Energy Research*, vol. 31, no. 1, pp. 14–28, 2007. [[CrossRef](#)] [[Google Scholar](#)] [[Publisher Link](#)]
- [21] Lalatendu Pattanayak, Jaya Narayan Sahu, and Pravakar Mohantye, "Combined Cycle Power Plant Performance Evaluation Using Exergy and Energy Analysis," *Environmental Progress & Sustainable Energy*, vol. 36, no. 4, pp. 1180-1186, 2017. [[CrossRef](#)] [[Google Scholar](#)] [[Publisher Link](#)]
- [22] Osman Shamet, Rana Ahmed, and Kamal Nasreldin Abdalla, "Energy and Exergy Analysis of a Steam Power Plant in Sudan," *African Journal of Engineering & Technology*, pp. 1-13, 2021. [[CrossRef](#)] [[Google Scholar](#)] [[Publisher Link](#)]
- [23] Mohamed Elhelwa, Kareem Saad Al Dahmaa, and Abd el Hamid Attiaa, "Utilizing Exergy Analysis in Studying the Performance of Steam Power Plant at Two Different Operation Mode," *Applied Thermal Engineering*, vol. 150, pp. 285-293, 2019. [[CrossRef](#)] [[Google Scholar](#)] [[Publisher Link](#)]
- [24] Sanjay, "Investigation of Effect of Variation of Cycle Parameters on Thermodynamic Performance of Gas-Steam Combined Cycle," *Energy*, vol. 36, no. 1, pp. 157-167, 2011. [[CrossRef](#)] [[Google Scholar](#)] [[Publisher Link](#)]
- [25] Fouad Khaldi, and Belkacem Adouane, "Energy and Exergy Analysis of a Gas Turbine Power Plant in Algeria," *International Journal of Exergy*, vol. 9, no. 4, pp. 399-413, 2011. [[CrossRef](#)] [[Google Scholar](#)] [[Publisher Link](#)]
- [26] H.Y. Kwak, D.J. Kim, and J.S. Jeon, "Exergetic and Thermo-economic Analyses of Power Plants," *Energy*, vol. 28, no. 4, pp. 343–360, 2003. [[CrossRef](#)] [[Google Scholar](#)] [[Publisher Link](#)]
- [27] Tadeusz Jozef Kotas, *The Exergy Method of Thermal Plant Analysis*, London: Butterworths, pp. 1-296, 1985. [[Google Scholar](#)] [[Publisher Link](#)]
- [28] Michael J. Moran, and Howard N. Shapiro, *Fundamentals of Engineering Thermodynamics*, New York: Wiley, pp. 1-918, 2000. [[Google Scholar](#)] [[Publisher Link](#)]
- [29] Borgnakke Claus, and Richard Edwin Sonntag, *Fundamentals of Thermodynamics*, 7<sup>th</sup> ed., John Wiley & Sons, pp. 1-800, 2009. [[Google Scholar](#)] [[Publisher Link](#)]
- [30] P.K. Nag, *Power Plant Engineering*, McGraw Hill Education, pp. 1-950, 2008. [[Google Scholar](#)] [[Publisher Link](#)]